Development 135, 2797-2805 (2008) doi:10.1242/dev.018341

BMP2 and BMP7 play antagonistic roles in feather induction

Frederic Michon[1], Loïc Forest[2,*], Elodie Collomb[1], Jacques Demongeot[2] and Danielle Dhouailly[1,†]

Feathers, like hairs, first appear as primordia consisting of an epidermal placode associated with a dermal condensation that is necessary for the continuation of their differentiation. Previously, the BMPs have been proposed to inhibit skin appendage formation. We show that the function of specific BMPs during feather development is more complex. *BMP2* and *BMP7*, which are expressed in both the epidermis and the dermis, are involved in an antagonistic fashion in regulating the formation of dermal condensations, and thus are both necessary for subsequent feather morphogenesis. *BMP7* is expressed earlier and functions as a chemoattractant that recruits cells into the condensation, whereas *BMP2* is expressed later, and leads to an arrest of cell migration, likely via its modulation of the EIIIA fibronectin domain and α4 integrin expression. Based on the observed cell proliferation, chemotaxis and the timing of *BMP2* and *BMP7* expression, we propose a mathematical model, a reaction-diffusion system, which not only simulates feather patterning, but which also can account for the negative effects of excess BMP2 or BMP7 on feather formation.

KEY WORDS: Dermis, Cutaneous appendage, Chemotaxis, Migration, Fibronectin, Mathematical model, Skin

INTRODUCTION

The integument is one of the most favorable organs for the study of how regular repetitive structures can arise during development within an ensemble of apparently identical cells. In vertebrates, as opposed to in other metazoans where the integument is composed of a single stratum of ectodermal cells, the situation is complicated by the fact that the skin is formed by two tissues, the epidermis and the dermis. In amniotes, the skin is equipped with cutaneous appendages, constituted of epidermal cells, that arise from the morphogenetic collaboration of dermis and epidermis (Dhouailly, 1977; Dhouailly, 1984), and these are distributed in an orderly fashion according to regional and specific patterns. The major part of our current knowledge of the establishment of skin patterns comes from studies of the chick embryo.

Chick skin can be divided into several domains: pterylae (feather field), semi-apteria (region with a few feathers) and apteria (glabrous area) (Mayerson and Fallon, 1985; Sengel, 1976). The future pterylae are characterized by the formation of a homogeneous, dense dermis (Sengel, 1976). In the back, this occurs from days 5 to 6.5 of incubation (stages HH25 to HH29) (Hamburger and Hamilton, 1951), and at day 7 (HH30) the midline, where the first row of feathers will appear, undergoes a further density increase. Before cell migration occurs to form individual dermal condensations, cells proliferate up to a threshold of 2.6 nuclei/1000 μm^3 (Desbiens et al., 1991; Jiang and Chuong, 1992; Wessells, 1965). By contrast, in semi-apteria the cell density remains under this threshold, reaching only up to 2.0 nuclei/1000 μm^3 (Olivera-Martinez et al., 2001). We have shown previously (Michon et al., 2007) that when cell density exceeds the threshold, proliferation stops and there is a redistribution of cells to form dermal condensations, where the cell density reaches 5.52 nuclei/1000 μm^3 (Wessels, 1965). These dermal condensations arise under the epidermal placodes. These two structures form the feather primordium, and the lateral propagation of this process creates a hexagonal feather pattern.

Several signaling pathways (Chuong, 1998) have been implicated in the crosstalk between the epidermis and the dense dermis that leads to feather morphogenesis. The exact sequence of events, in the narrow time window available for primordium formation, is not yet clear. The different signals have been classified as activators or inhibitors (Jung et al., 1998). The FGF pathway acts as an activator, and its epidermal expression promotes dermal condensation formation via its chemoattractant effect on fibroblasts (Song et al., 1996; Song et al., 2004; Viallet et al., 1998). To date, BMPs have generally been considered to be inhibitors of feather formation, and three members are expressed in the primordium domain: BMP2, BMP4 and BMP7, where BMP2 and BMP4 belong to the same subgroup (Miyazono et al., 2005). *BMP2* is initially expressed throughout the epidermis, but is later restricted to placodes and appears in dermal condensations (Noramly and Morgan, 1998). *BMP4* transcripts are detected only in the forming dermal condensations (Noramly and Morgan, 1998). *BMP7* is expressed throughout the epidermis before placode formation and is subsequently restricted to the primordium, in both dermis and epidermis (Harris et al., 2004). *BMP2* expression occurs earlier than *BMP4* (Houghton et al., 2005), and later than *BMP7* (Harris et al., 2004). The transcriptional regulation of *BMP2* and *BMP4* expression in embryonic skin is still unknown. *BMP7* is expressed in the epidermis under the control of an unknown dermal signal, whereas its dermal expression is regulated by canonical Wnt signaling derived from the placode (Harris et al., 2004).

Studies designed to evaluate the function of BMPs in developing skin have provided incongruous data. The BMP pathway has been demonstrated to function as an inhibitor of feather (Jung et al., 1998), as well as of hair (Botchkarev, 2003) and tooth (Pummila et al., 2007), formation, under certain experimental conditions. BMP4-coated beads grafted onto chick HH28 (E6) dorsal skin inhibits adjacent feather formation (Jung et al., 1998), and *BMP4* overexpression in chick embryo dorsal skin leads to the formation of glabrous areas (Noramly and Morgan, 1998). However, the other pieces of evidence are contradictory. The application of BMP7-

[1]Equipe Ontogenèse et Cellules Souches du Tégument, Centre de Recherche INSERM UJF – U823, Institut Albert Bonniot, Site Santé, La Tronche, BP170, 38042 Grenoble Cedex 9, France. [2]Laboratoire de Techniques de l'Imagerie, de la Modélisation et de la Cognition UMR CNRS 5525, Institut d'Informatique et de Mathématiques Appliquées de Grenoble, Faculté de Médecine, 38706 La Tronche, Cedex, France.

*Deceased
†Author for correspondence (e-mail: Danielle.Dhouailly@ujf-grenoble.fr)

Accepted 19 June 2008

coated beads inhibits feather formation (Patel et al., 1999), although its epidermal expression has been shown to be required (Harris et al., 2004). An ectopic feather-forming dermis can be obtained in two opposite ways: by the inhibition of BMP signaling in the mid-ventral apterium (Fliniaux et al., 2004), or by grafting a BMP4-coated bead into the dorsal-scapular semi-apterium (Scaal et al., 2002). These contradictory results might be explained by spatial factors, as the molecular mechanisms responsible for the establishment of the dermis in the back and the ventral region are different (Fliniaux et al., 2004; Olivera-Martinez et al., 2002). Moreover, for the back region, whereas the use of low concentration BMP4-coated beads (20 μg/ml) (Scaal et al., 2002) leads to activation of feather formation, RCAS-BMP4 infection (Noramly and Morgan, 1998) or the use of high concentration BMP4-coated beads (660 μg/ml) (Jung et al., 1998) leads to an inhibitory effect. Additionally, some results suggest an activator role for BMP signaling. *MSX1* and *MSX2*, two BMP target genes, are expressed in the placode (Noveen et al., 1995). *DRM*/gremlin (BMP signaling antagonist) transcripts are restricted to the interfollicular domain (Bardot et al., 2004), and although follistatin (another BMP signaling antagonist) expression initially occurs throughout the placode, it rapidly shifts to a peripheral ring (Patel et al., 1999). Altogether, the expression of BMP target genes and the absence, or the transient expression, of BMP inhibitors in the follicular domain, as well as the importance of the concentration of the BMP delivered experimentally, indicate a complex role for the BMPs in feather morphogenesis.

In order to distinguish the different roles of BMP signaling in chick embryonic skin, we examined three different aspects. First, we investigated the expression of another set of downstream targets of BMP signaling, the ID genes (Hollnagel et al., 1999), thought to inhibit cell differentiation (Kreider et al., 1992; Miyazono and Miyazawa, 2002; Ogata et al., 1993). In chick, four ID genes have been identified (Kee and Bronner-Fraser, 2001), but we describe their expression in skin. Second, we studied in vitro dermal fibroblast behavior in response to different BMPs. Both fibroblast migration (Mauger et al., 1982) and Fibronectin (Chuong, 1993; Michon et al., 2007) have been implicated in the transition from a dense dermis to individual dermal condensations. Alternative splicing of the fibronectin gene has been identified as a key regulator of Fibronectin/Integrin affinity in CHO cells (Manabe et al., 1997). Furthermore, by promoting adhesion on α5β1 Integrin, the Fibronectin EIIIA domain was shown to induce the G1-S transition (Manabe et al., 1999). We thus studied the changes in fibronectin EIIIA domain expression during dermal organization. Finally, we established, in silico, a mathematical model based on an activation/inhibition-diffusion Turing system (Turing, 1952), which takes into account the parameters of cell density and migration.

We show that instead of acting as 'inhibitors', different BMPs play distinct crucial roles, ranging from the regulation of dermal condensation formation to the continuation of feather morphogenesis. Furthermore, our numerical simulation is not only in agreement with our biological experimental results, but also provides an explanation for apparently contradictory results (Jung et al., 1998; Noramly and Morgan, 1998)

MATERIALS AND METHODS

Materials

Fertilized eggs (JA957 strain, St Marcellin, France) were incubated for seven days at 38°C until the embryos reached Hamburger Hamilton stage 29 or 30 (Hamburger and Hamilton, 1951). rhBMP2, rhBMP7 and rhFGF2 were purchased from R&D Systems, Europe.

Organotypic skin in vitro culture

Seven-day chick embryo (stage HH29 or 30) dorsal skins were dissected as a single piece, starting from the wing to the femoral level. They were cultured as previously described (Michon et al., 2007). For localized application, 150 to 200 μm diameter Affi-gel Blue beads (Bio-Rad) were soaked in PBS or rhBMP7 (concentrations specified in figure legends) and then placed onto the explants.

Dermal fibroblast in vitro culture

The dermis was separated from the epidermis by treatment with Trypsin (1.25%) and Pancreatin (4%, Sigma-Aldrich), then was mechanically dissociated into a single-cell suspension. Cells were used for RT-PCR, adherent cell culture, cell migration assay or micromass formation. To evaluate cell migration, 2.5×10^4 cells were used for each experimental condition using the Innocyte cell migration assay (VWR International) (Lauffenburger, 1996). Migration was measured after 10 hours by Calcein-AM dye. Fetal Bovine Serum was used as an attraction factor for cells as a positive control. Micromass culture was performed as described previously (Michon et al., 2007).

FACS analysis

HH29 and HH30 chick embryo dorsal skins were dissected into separate medial and lateral parts. Obtained dermal cell suspensions were fixed in cold ethanol (2×10^6 cells/ml). Cell aggregates were broken up mechanically and cells were labeled in 0.1% NP40, 0.1 mg/ml RNAse A, 50 μg/ml Propidium Iodide (Sigma). Cells were rinsed in PBS and FACS analysis was performed using Cell Quest Pro software (Becton Dickinson).

Molecular biology

RNA was isolated with the High Pure RNA tissue kit (Roche). Reverse transcription was performed with the SuperScript First-Strand synthesis system (Invitrogen). PCR products were analyzed with Image J software (NIH). Primers used were: cActin sense, AGACCTTCAACACCCCAGC; cActin antisense, TGATTTTCATTGTGCTAGG; cEIIIA sense, ATGGTACAGCGTCTATGCTCA; cEIIIA antisense, AGACTGGTAGGAGTTACCTGA; Fibronectin sense, CAGTGGCTACCGAGTGACCAC; Fibronectin antisense, AGACTGGTAGGAGTTACCTGA. Primers for chick Actin were designed to discriminate between genomic and complementary DNA (926 bp versus 619 bp).

In situ hybridization

The chick *EIIIA* probe was cloned into the pGEM-T Easy vector (Promega, France) [based on its published sequence (Norton and Hynes, 1987)]. The *cBMP2* and *cBMP7* probes were a gift from Dr A.-H. Monsoro-Burq (Centre Universitaire, Orsay, France). The chick follistatin probe was a gift from Dr A. Graham (King's College London, UK). The *cID1*, *cID3*, *cID4* and cα4 integrin probes were a gift from Dr M. Bronner-Fraser (University of California, Irvine, CA, USA). Alkaline phosphatase-labelled in situ hybridizations were carried out as previously described (Wilkinson and Nieto, 1993).

RESULTS

Sequential expression of BMPs, follistatin and ID genes in early feather primordium

As the two femoral feather tracts of the same embryo develop synchronously on the left and right sides, we used them to compare the timing of expression of two genes (Houghton et al., 2005). Feather rows were numbered according to the order of appearance. The femoral tract has seventeen rows, fifteen proximal to the first one. Distal to the first row, a discontinuous line of expression that gives rise to the third row occurred. This third row forms the boundary between the femoral and zeugopodial tracts, which are on each side of a semi-apteria. The expression of *BMP2* and *BMP7* in corresponding feather primordia of the left and right halves of the same embryo were compared at HH30 (n=6/6 for each comparison). In the second row of this tract, *BMP2* was expressed in only two primordia (Fig. 1A), whereas BMP7 was expressed in

DEVELOPMENT

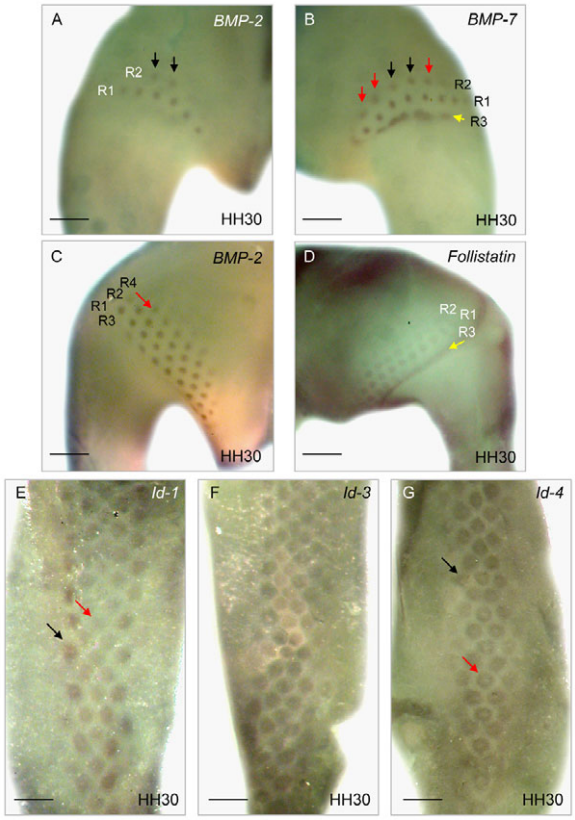

Fig. 1. The expression of BMP pathway factors during feather primordium formation. (**A-D**) The left and right femoral tract of the same HH30 embryo were compared; the numbers correspond to the order of appearance of the rows. The second row (R2) had only two feather primordia expressing *BMP2* (A), whereas five expressed *BMP7* (B). The additional primordia are indicated with red arrows and those also expressing *BMP2* with black arrows. The distal border (yellow arrow), which preceded the appearance of R3, delimited the femoral and zeugopodial tracts and already expressed *BMP7* (B) but not *BMP2* (A). In another embryo, R4 expressed *BMP2* on the left side (C, arrow), whereas follistatin was expressed only in three rows on the right (D). The continuous line (D, arrow), contiguous to R3, is the distal border of the tract, which expressed follistatin and not *BMP2*. (**E-G**) ID gene expression in the dorsal tract of HH30 embryos, analyzed by in situ hybridization with RNA probes. (E) There was a decrease of *ID1* expression from the newly formed (black arrow) to the older primordia (red arrow). (F) *ID3* transcripts showed stable expression in all the primordia. (G) *ID4* expression exhibited early expression in the entire primordia (black arrow), and later expression restricted to a peripheral ring (red arrow). Scale bars: in A-D, 1000 μm; in E-G, 800 μm.

five (Fig. 1B). Follistatin (Fig. 1D), a BMP inhibitor, was expressed after *BMP2* (Fig. 1C). The *ID1*, *ID3* and *ID4* transcripts were detected in HH30 dorsal skin in the primordia (Fig. 1E-G). *ID4* expression appeared initially in the complete primordium (newly formed rows), but subsequently the transcripts were detected only as a peripheral ring (Fig. 1G). The expression of *ID1* and *ID4* was concomitant to that of *BMP2* (see Fig. S1A-D in the supplementary material), and the expression of *ID3* was concomitant to that of *BMP7* (see Fig. S1E,F in the supplementary material). These data indicate that the BMP pathway is actively involved in feather formation.

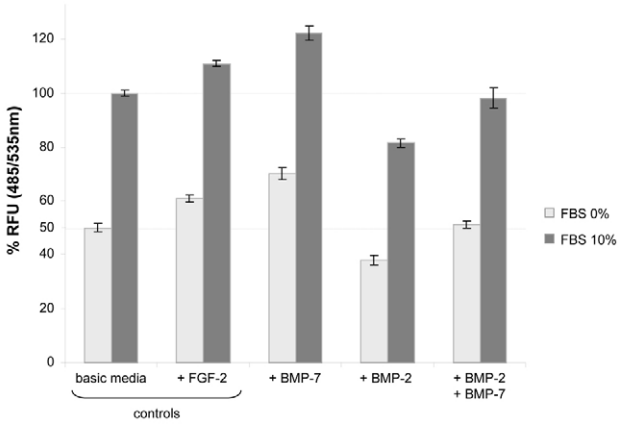

Fig. 2. Comparative effects of BMP2 and BMP7 on dermal fibroblast cytokinesis. A freshly dissociated dermal cell suspension was added to a cell culture insert and basic medium placed on the other side of the 8 μm pore membrane. Two types of control were performed: first, basic media with or without FBS; and second, basic media with or without FBS, with FGF2. The first control allowed a normalization of the cell migration measurement (50.1% and 100%), the second, the validation of the chemotactic effect with FGF2 (60.8% and 110.9%). BMP7 had an even stronger chemotactic effect (70.1% and 122.3%). Perturbation of fibroblast migration was clearly shown with BMP2 (38.1% and 81.6%). The chemotaxis obtained with BMP7 decreased with the addition of BMP2 (51.2% and 98.2%). The migration was evaluated in triplicate by a fluorescent method. $P<0.05$ by Student's *t*-test. BMP2 and BMP7, 0.5 μg/ml; FGF2, 0.33 μg/ml.

BMP2 and BMP7 have opposite effects on dermal fibroblast migration

In order to distinguish the relative roles of BMP2 and BMP7, we quantified their effects on fibroblast migration through a membrane under various conditions (Fig. 2). Two kinds of controls were performed. First, we used the basic medium with or without 10% Fetal Bovine Serum (FBS), which has a known chemoattractant effect. Secondly, we added FGF2, which is known to have a positive chemoattractant effect on dermal cells (Song et al., 2004), to the basic media with or without FBS. Each experiment, done in triplicate, was measured relative to the cell migration obtained with the basic medium containing FBS (100%). Without FBS, cell migration decreased to 50.1% ($P<0.001$). FGF2 activated cell motility, in both the presence (+11.9%, $P<0.01$) and the absence (+10.7%, $P<0.01$) of FBS. Interestingly, BMP7 had an even stronger effect than did FGF2 in the presence (+22.2%, $P<0.01$) and the absence (+20%, $P<0.01$) of FBS, whereas BMP2 had an inhibitory effect on migration: –18.7% ($P<0.01$) with and –11.9% ($P<0.01$) without FBS. Combining BMP2 and BMP7 in the same medium cancelled out the effect of each factor on dermal cell migration. The difference between the chemotactic effect of both BMPs and that of only BMP7 was striking: –24.1% ($P<0.02$) with and –18.9% ($P<0.01$) without FBS. Our in vitro assay was independent of extracellular matrix, but, in vivo, there might be interactions between it and the BMPs.

BMP2 modifies the expression of fibronectin EIIIA domain and α4 integrin

Analysis with the probe specific for the fibronectin EIIIA domain showed a lack of expression in fully formed dorsal skin dermal condensations at HH29+, although Fibronectin expression is high in this area (Chuong, 1993; Michon et al., 2007). Moreover, the

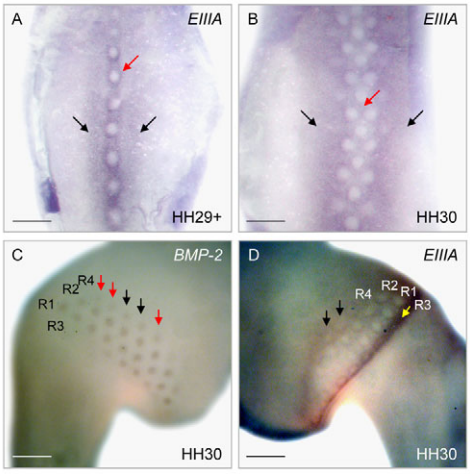

Fig. 3. The Fibronectin exon EIIIA was involved in dermal organization. (**A**,**B**) Chick embryo dorsal skin. (A) At HH29+, EIIIA was expressed in the periphery (red arrow) of the first feather primordia, as well as in two ribbons on either side of the first row (black arrows). (B) At HH30, the EIIIA transcripts were expressed in the periphery of primordia and in two ribbons (black arrows) on either side of feather rows, although there was a slight decrease of its expression in the three first rows (red arrow). (**C**,**D**) *BMP2* and EIIIA expression in the left and right femoral tract of the same HH30 embryo. Five feather primordia of the fourth row (R4) expressed *BMP2* (C), whereas two no longer expressed EIIIA in the corresponding right row (D). The additional primordia are indicated with red arrows and those no longer expressing EIIIA with black arrows. The R3, expressing the EIIIA domain (arrow) has started to form close to the distal border line. Scale bars: 800 μm in A,B; 1000 μm in C,D.

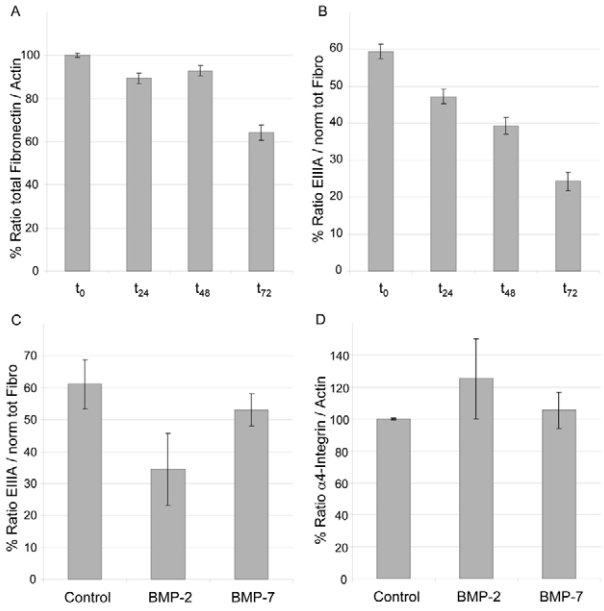

Fig. 4. The regulation of EIIIA and α4 integrin expression. (**A**,**B**) EIIIA expression in dermal fibroblasts cultured in hanging drops for 24, 48 or 72 hours. RT-PCR for Actin, total Fibronectin and the EIIIA exon were performed. Fibronectin expression was normalized to Actin expression. There was a small decrease in Fibronectin expression between t_0 (100%) and t_{48} (92.8%), and, a noticeable decrease at t_{72} (64.1%; A). EIIIA expression was normalized to Fibronectin expression. During the same time-lapse, the portion of Fibronectin-expressing cells containing the EIIIA exon decreased from 59.4% to 24.3% (B). (**C**,**D**) Cells were placed in adherent culture with or without BMP2 and BMP7 (0.5 μg/ml) for 20 hours. Then RT-PCR to detect EIIIA and integrin α4 expression was performed. The portion of Fibronectin-expressing cells containing the EIIIA exon decreased with BMP2 treatment, from 61.1% to 34.4%, whereas BMP7 treatment led to a slight decrease, 53.1% (C). BMP2 treatment led to an increase of α4 integrin expression, from 100% to 125.29%, whereas BMP7 induced only a non-significant increase (105.5%; D).

expression of the EIIIA domain was high in areas in which the dense dermis was still undergoing organization (Fig. 3A). At HH30, there was a lateral expansion of EIIIA domain expression and a slight decrease of its expression in the interfollicular domain of the first rows formed (Fig. 3B). To analyze in time the loss of the EIIIA domain transcripts, we compared its expression with that of *BMP2* (n=9/9). Whereas *BMP2* was expressed in five primordia on the fourth row (Fig. 3C), the loss of EIIIA expression occurred only in two of the primordia of the same row (Fig. 3D). Furthermore, strong expression was detected at the distal boundary of the tract close to the third row that has started to form. The expression of *BMP2* thus preceded the alternative splicing of the fibronectin EIIIA domain.

To study the alternative splicing of EIIIA, we used freshly isolated dermal cells in two complementary approaches. In order to mimic the formation of dermal condensations in vitro by dispersed fibroblasts, we used the micromass method (Michon et al., 2007) to follow cell aggregation for 3 days. Semi-quantitative RT-PCR (n=3) was performed in order to monitor fibronectin and fibronectin EIIIA expression (Fig. 4). There was a decrease of fibronectin expression from t_0 (100%) to t_{72} (64.1%; Fig. 4A), but the proportion of fibronectin containing the EIIIA exon had decreased more, from 59.4 to 24.3%, during the same time (Fig. 4B). The relative decrease of EIIIA domain expression was also induced in adherent cell culture via the addition of BMP2. Semi-quantitative RT-PCR of primary cultured dermal fibroblasts showed expression of the EIIIA domain after 20 hours of culture under control conditions, whereas the addition of BMP2 led to a decrease of EIIIA domain expression after 20 hours of treatment, from 61.1% to 34.4% (Fig. 4C). There was a slight effect caused by BMP7 treatment, from 61.1% to 53.1%.

α4 Integrin was expressed in the follicular domain (data not shown), and it was shown previously in the dermal condensation (Jaspers et al., 1995). The addition of BMP2 induced the overexpression of α4 integrin as well, from 100% to 125.3% (Fig. 4D). The addition of BMP7 led to a non-significant increase of α4 integrin expression. As the Fibronectin EIIIA domain was shown not only to modulate the Fibronectin/Integrin interaction, but also to be implicated in the control of cell proliferation (Manabe et al., 1999), we quantified the population of cycling cells in dorsal skin before and after dermal condensation formation.

Cell proliferation in the chick embryo dorsal skin at HH29 and HH30

Cycling cells have been localized previously in the interfollicular dermis and not in the formed dermal condensation (Rouzankina et al., 2004; Wessells, 1965). We studied cell proliferation during dermal condensation formation in chick embryo dorsal skin from HH29 to HH30. At these stages, dorsal skin can be divided into three parts: the medial part, carrying the first dermal condensation at HH30, and the two lateral parts (see Fig. S2A,B in the supplementary material). The proportion of cycling dermal cells

in each part was determined by flow cytometry (see Fig. S2C in the supplementary material). At HH29, the difference between the lateral and the medial parts was not significant. The slight decrease of cycling cells in the medial part might reflect the start of dermal condensation formation. At HH30, the central part of the dermis, where dermal condensations are forming, had 90.9% of cells in G1, whereas in the lateral part only 77.5% of cells were in G1. The proliferation of dermal cells just before condensation formation is likely to lead to the establishment of the required cell density.

Mathematical model for dermal condensation formation and patterning

Our results have allowed us to build a new mathematical model for feather primordia formation that includes cell proliferation and cell migration, regulated by BMP7 and BMP2 expression. The model for BMP dynamics was inspired by the activator-inhibitor model proposed by Gierer and Meinhardt (Gierer and Meinhardt, 1972). Cell migration is expressed as a chemotactic term, as in previous studies (Cruywagen et al., 1992; Painter et al., 1999). BMP7 is an activator of feather primordium formation through its effect on chemotaxis and cell recruitment, whereas BMP2 counteracts the positive effect of BMP7 on cell migration. Another important issue is that the model can be run from initial conditions consistent with the in vivo situation in the chick embryo dorsal skin at HH29.

The mathematical model describes the spatiotemporal dynamics of four variables: n_1 n_2, u and v in a two-dimensional space Ω. The dermal cell population, whose concentration is noted n ($n=n_1+n_2$), was divided into two subpopulations: n_1 (cycling cells) and n_2 (migrant cells). u and v represent the concentration and the cellular effect, respectively, of BMP7 and BMP2.

Cellular dynamics

The proliferation of n_1 cells is modeled by a logistic growth function, where k_p is the proliferation constant and N the maximal cell population. n_1 cells proliferated until they reached a threshold of cell density n^* at the time t^*. After the concentration overcame the threshold, n_1 cells progressively stopped proliferating and acquired the ability to migrate. This transition is determined by a 'differentiation' constant k_d (taken as being equal to k_p in the following). For n_2 cells, the migration flux was modeled by a diffusive part with constant D_n and a chemotaxis part with a constant χ. The chemoattractant is u.

Equations for n_1 and n_2 are:

$$\frac{\partial n_1}{\partial t} = \begin{cases} k_p n_1 \left(N - n_1\right) & \text{if } t \leqslant t^* \\ -k_d n_1 & \text{else} \end{cases} \quad (1)$$

$$\frac{\partial n_2}{\partial t} = D_n \Delta n_2 - \nabla.\left(\chi n_2 \nabla u\right) + \begin{cases} 0 & \text{if } t \leqslant t^* \\ k_d n_1 & \text{else} \end{cases} \quad (2)$$

$n_{1,0}$ and $n_{2,0}$ are the initial conditions for n_1 and n_2. No flux boundary condition is used for n_2.

BMP dynamics

u and v dynamics have been given by reaction-diffusion equations. D_u and D_v denote the respective diffusion constants. Reaction terms were made of a linear degradation part (with constants k_u and k_v) and a production part. The production part for each chemical was constructed so as to respect the qualitative regulation between them. As they are synthesized by n_2 cells, production terms are also taken proportional to n_2. We have:

$$\frac{\partial u}{\partial t} = D_u \Delta u + \frac{c_1 n_2 \left(1 + c_2 u^2\right)}{\left(c_3 + u^2\right)\left(1 + v\right)} - k_u u \quad (3)$$

$$\frac{\partial v}{\partial t} = D_v \Delta v + c_4 n_2 u^2 - k_v v \quad (4)$$

c_1, c_2, c_3 and c_4 are positive constants.

Production terms stated that *BMP7* expression was reinforced by a 'spot' (dermal condensation) microenvironment. For v=0: (1) for small values of u, the secretion rate σ of BMP7 was proportional to the number of n_2 secreting cells ($\sigma=c_1 n_2/c_3$); (2) for medium values of u, σ followed Hill kinetics, with autocatalyse of cooperativity 2 by BMP7 ($\sigma=c_1 c_2 n_2\, u^2/(c_3+u^2)$); and (3) for high values of u, autocatalyse saturated and σ was proportional to n_2 ($\sigma=c_1 c_2 n_2$). For v>0, BMP2 was a competitive inhibitor of BMP7, and both *BMP2* and *BMP7* were expressed by the same cell population (primordium domain). Initial conditions for u and v are given by u_0 and v_0, which are generally taken as being equal to 0. No flux boundary conditions are used for u and v.

Resulting model

The simple dynamics for n_1 cells allows the exact computation of $n_1(x,y,t)$, where (x,y) are the 2D-space coordinates. If n^* is defined as a fraction Q of the maximal cell density N, $n^*=QN$, we have:

$$n_1\left(x,y,t\right) = \frac{N n_{1,0}\left(x,y\right) e^{Nk_d t}}{N + n_{1,0}\left(x,y\right)\left(e^{Nk_d t} - 1\right)} \quad (5)$$

for $t \leqslant t^*(x,y)$, and then $n_1(x,y,t)=n^*\, e^{Nk_d(t-t^*)}$ if Q is small, and $n_1(x,y,t)=n^*\, e^{Nk_d(t-t^*)}/(1-Q+Qe^{Nk_d(t-t^*)})$, if Q is large. $t^*(x,y)$ is given by:

$$t^*\left(x,y\right) = \frac{1}{Nk_d} \ln\left(\frac{Q\left(N - n_{1,0}\left(x,y\right)\right)}{n_{1,0}\left(x,y\right)\left(1 - Q\right)}\right) \quad (6)$$

This allows directly expressing the production term of n_2 cells as a delayed production term and reducing the model as follows:

$$\begin{cases} \dfrac{\partial n_2}{\partial t} = D_n \Delta n_2 - \nabla.\left(\chi n_2 \nabla u\right) + \begin{cases} 0 & \text{if } t \leqslant t^* \\ k_d n^*\, e^{k_d\left(t - t^*\right)} & \text{else} \end{cases} \\ \dfrac{\partial u}{\partial t} = D_u \Delta u + \dfrac{c_1 n_2 \left(1 + c_2 u^2\right)}{\left(c_3 + u^2\right)\left(1 + v\right)} - k_u u \\ \dfrac{\partial v}{\partial t} = D_v \Delta v + c_4 n_2 u^2 - k_v v \end{cases} \quad (7)$$

and reducing the model as equations 2, 3, 4, in which n_1 is replaced by its expression above in terms of n^* and t^*.

Numerical simulations

The calculations were made using the software COMSOL Multiphysics 3.2 and the finite elements method using squared meshes. We took Ω=]–1.1[×]0.1[and the parameters given in Table S1 (see supplementary material).

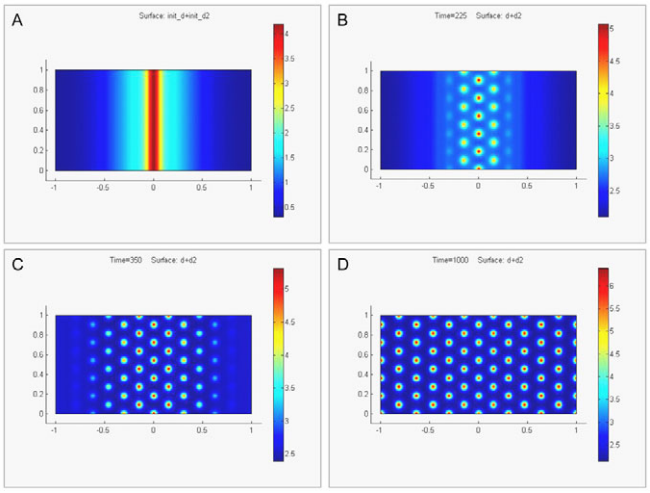

Fig. 5. Sequential appearance and patterning of spots with mathematical simulation. (**A**) The resolution of the model led to the formation of a primary migrating cell midline. (**B**) The redistribution of these cells, via chemotaxis, led to the formation of spots, whereas laterally, new cells started to migrate. (**C**) The lateral expansion of the pattern was due to migrating cells under both chemotaxis and arresting factors. (**D**) At the end of the simulation, the hexagonal pattern occurred all over the modeled domain. Cell density is represented in false colors.

For the sequential spots appearance numerical experiment, the initial situations for n_1 and n_2 are given by: $n_{1,0}(x)=0.25+1.7\exp(-5x^2)+0.2\exp(-200x^2)$ and $n_{2,0}(x)=0.05+2\exp(-200x^2)$. All other initial values are set to 0. Pulse experiments are realized using the same initial situation. Pulses are modeled by additional production terms in the equation of BMP7 or BMP2. For the local pulse of BMP7 experiment, equation 3 becomes equation 3′:

$$\frac{\partial u}{\partial t} = D_u \Delta u + \frac{c_1 n_2 \left(1 + c_2 u^2\right)}{\left(c_3 + u^2\right)\left(1 + v\right)} - k_u u + p_u \qquad (8)$$

where $p_u(x,y)=25\exp(-500(x^2+(y-0.5)^2))$. This expression of the additional term allows the specification of sharp pulse located in the centre of the domain. For the global pulse of BMP2 we used the new term: $p_v=700$, and equation 4 becomes equation 4′:

$$\frac{\partial v}{\partial t} = D_v \Delta v + c_4 n_2 u^2 - k_v v + p_v \qquad (9)$$

To investigate the impact of cell density on the pattern, we ran the model from initial situations in which n_2 cells are homogeneously distributed in the domain with a density q, affected by small random fluctuations. n_1 cells are not represented. Patterns are observed at the same time t=1000.

Dermal condensation formation obtained with numerical resolution

The result of running the simulation was the formation of a pattern of spots that closely resembles the in vivo feather pattern: a medial first row followed by the lateral formation of new rows leading to a hexagonal pattern (Fig. 5A-D; see also Movies 1 and 2 in the supplementary material). Based on previous observations of our laboratory (Olivera-Martinez et al., 2001), we included the cell densities in the dermis of apterium, semi-apterium and pteryla

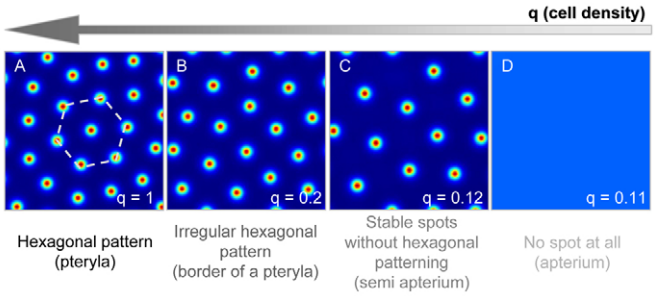

Fig. 6. The progressive increase of the cell density correlated successively with the formation of an apterium, a semi-apterium and a pteryla. (**A**) The pteryla was characterized by a regular pattern. (**B**,**C**) The decrease of cell density (q) to 0.2 (B) and 0.12 (C) led, respectively, to an irregular pattern at the boundary of the pteryla and the semi-apteria. (**D**) The switch from spot formation to a glabrous region implicated only a small difference in cell density (q=0.12 versus q=0.11).

before and during the primordium formation in the model parameters. For the formation of a hexagonal pattern, the cell density threshold (N=2.6) and its repartition between primordium (n=5.5) and interfollicular (n=1.5) was in accordance with the in vivo observations. For the feather tract formation, a cell density threshold (q=1) was required (Fig. 6A). Under this threshold (q=0.2 to 0.12), the pattern formation was irregular (Fig. 6B,C), similar to what is observed in semi-apteria. The cell density limit was obtained with q=0.11, where no spots were formed (Fig. 6D), similar to what occurs in apteria.

The increase of activator, like that of inhibitor, led to spot inhibition

Using our mathematical model, an increase of the local pulse concentration of activator led to the increase of cell recruitment under the source according to the chemoattractant effect, resulting

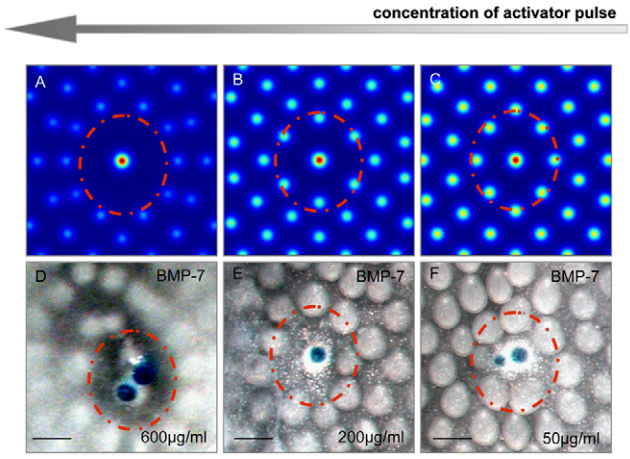

Fig. 7. The over-activation of chemoattraction led to similar results with mathematical simulation and organotypic culture. (**A-C**) Simulation of a local pulse of activator led to the formation of an accumulation of cells, surrounded by a ring of inhibition. The size of this ring was proportional to the activator concentration. (**D-F**) Patterns resulting from the local application of BMP7-coated beads. The maximal area of inhibition (red circle) was obtained with the maximal concentration of BMP7. $p_u(x,0)=c*\exp(-(x^2+(y-0.5)^2)*500)$ with c=4, 8 or 24. Scale bars: 250 µm.

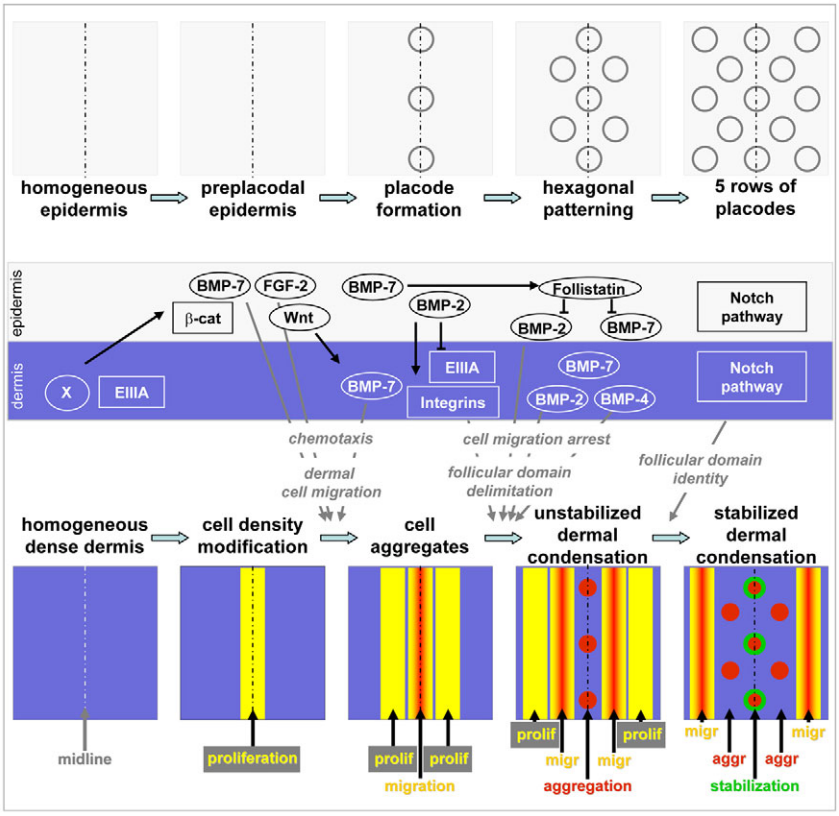

Fig. 8. Model of dermal condensation formation in dorsal chick embryo skin. The chronological events from dense dermis to stabilized dermal condensation require a molecular dialogue both inter- and intra-tissular in the skin (see the text). Note that the placodes are larger and earlier than the dermal condensations (Dhouailly, 1984). This model took into account only the BMP genes, as well as a few other important genes among those expressed in embryonic skin.

in an area of lower cell density around the source, which could not support the formation of spots. The inhibition of spot formation followed the overactivation of cell recruitment, but the pattern was maintained beyond this circle of depleted cell density (Fig. 7A-C; see also Movies 3 and 4 in the supplementary material). This result has been also obtained in vitro (Fig. 7D-F). The diameter of the circle lacking the formation of dermal condensations was augmented by the application of BMP7 beads loaded with increasing concentrations, presumably because of the chemoattractant effect of BMP7. The highest concentration of BMP7 used (600 μg/ml) dramatically affected feather patterning.

By increasing the concentration of the inhibitor pulse (see Fig. S3A-C in the supplementary material), our model also mimicked previous in vivo results. The area of inhibition, caused by the arrest of cell migration, increased with the inhibitor concentration, as previously described with BMP2-coated beads (Jung et al., 1998). It also mimicked the results obtained by a global pulse of overactivation in RCAS-BMP2/BMP4 experiments (Noramly and Morgan, 1998).

DISCUSSION

The expression of BMP target genes, such as *ID1*, *ID3* and *ID4*, as shown here, or *MSX1* and *MSX2* as previously shown (Chuong et al., 1996), indicates that positive effects of the BMP pathway are required for feather morphogenesis. We propose antagonistic roles for BMP7 and BMP2, during feather primordium formation. BMP7 appears to act as a chemoattractant factor for dermal fibroblasts, this effect of BMP7 has also been described on human mesenchymal stem cells (Lee et al., 2006). BMP2, which is expressed later, appears to arrest the migration, slowing down cell recruitment to the condensation. The later expression of BMP4 in the dermal condensation (Noramly and Morgan, 1998) could also act in the arrest of cell migration because of its redundant activity with BMP2. As previously suggested in the osteogenic differentiation (Hazama et al., 1995), the concomitant presence of *BMP2*, *BMP4* and *BMP7* modifies the effect of each factor on cell migration. We propose the BMP pathway as regulator of both the formation of the dermal condensation, and the expression of ID and MSX genes, which allows the continuation of feather morphogenesis.

The different effects of BMP7 versus BMP2 and BMP4 appear linked to the activation of different receptors. BMP7 activity is mediated by its binding to Activin type I (ACTRI) (Miyazono, 1999) and type II (ACTRII) (Sebald and Mueller, 2003) receptors. A direct link between Activin receptor (ACTR) activation and cell migration has been proposed in keratinocytes (Zhang et al., 2005). These mechanisms involve Rho-GTPases, which are required for fibroblast migration (Michon et al., 2007). By contrast, BMP2/BMP4 activity is mediated by their binding to BMP type I and II receptors (Botchkarev, 2003). Infection with a RCAS dominant-negative type I BMP receptor in the prospective chick hindlimb resulted in the growth of feathers on scales (Zou and Niswander, 1996). We suggest that the enhancement of the dermal condensation, which was not limited by BMP2 signaling, was the key factor. BMP2 might negatively affect cell migration in at least three manners. First, because BMP2 in our in vitro experiments regulated the alternative splicing of the EIIIA domain of Fibronectin, we suggest that it might have a similar role in vivo. Although there is an increase of Fibronectin deposition in the dermal condensation (Mauger et al., 1982; Michon et al., 2007), the fibronectin EIIIA domain is spliced out in this area. Indeed, the skin expression pattern of EIIIA reflects the state of dermal organization: cell migration (EIIIA expression), or the formation of dermal condensations (loss of *EIIIA* expression). Second, BMP2 might regulate cell migration

via a direct effect on integrin expression. Here, we showed an upregulation of α4 integrin expression. Likewise, BMP2 modulates the expression of β1 integrin in osteoblasts (Sotobori et al., 2006), or of α2 and α7 integrin in satellite cells (Ozeki et al., 2007). This direct link between BMP2 and integrin expression could explain the rapid effect on primary dermal cells that we observed in our cell migration assay. Finally, the loss of EIIIA in dermal condensation correlates, as has been previously shown in other organs (Manabe et al., 1999; Manabe et al., 1997), with the absence of cycling cells in dermal condensations (Jiang and Chuong, 1992; Wessells, 1965), and could thus reflect an indirect role for the BMP2 pathway on cell cycle regulation. Altogether, the expression of *BMP2* in dermal condensations could trigger both the arrest of dermal cell migration, through the modulation of adhesion factors, and the arrest of cell proliferation.

Consistent with these processes, we propose a mathematical model that includes cell proliferation and cell migration by chemotaxis, but that is still far less intricate than is reality. It is a single layer model that does not take into account the first epidermal *BMP7* impulse or its role in the stabilization of the formed structures, or a potential heterodimerization between the BMPs. In our model, we have attributed a chemoattractant role to BMP7 and an arrest role to BMP2. It closely mimics the sequential hexagonal pattern formation observed in vivo, and clarifies the relation between cell densities and spot formation, which was hinted at in previous in vitro experiments (Jiang et al., 1999). Moreover, we showed that the difference in cell density that is required to switch from the formation of spots to a glabrous area is small (9%). Our mathematical model can also explain previous biological results, which concluded that BMP factors act as inhibitors. The use of a point source of a high concentration of activator, which induces an over-recruitment of cells, creates an area without the required cell density for dermal condensation formation, and thus mimics the nude area around a BMP7-coated bead, which was previously interpreted as an inhibitory effect (Patel et al., 1999). Our model explains this result as an over-activation of chemotaxis. Other biological results that were reproduced by our model are RCAS-BMP2 skin infection (Noramly and Morgan, 1998), the use of BMP2-coated beads (Jung et al., 1998), and the addition of BMP2 in the culture medium (our experiments). All of these methods led to the homogeneous overactivation of BMP2 in areas that then stay glabrous. Our simulation showed that a local or a homogeneously high concentration of the factor that arrests cell migration led to the formation of a glabrous area. Our model can also partially explain the effects of FGF4-coated beads on chick skin, i.e. the appearance of the typical small inhibition ring around the bead (chemotaxis), but not the feather bud fusions (Jung et al., 1998; Widelitz et al., 1996).

Finally, we propose a new view of BMPs and dermis organization, which is consistent with previous results, although not with their interpretations. It consists of three major steps: dermal cell migration, follicular domain delimitation, and the establishment of follicular domain identity (Fig. 8). Initially there is a limited proliferation along the dorsal midline until a critical cell density is obtained. Then, the molecular dialogue between the epidermis and the dermis, which leads to primordium formation, initiates. Activation of β-catenin in the epidermis (Noramly et al., 1999) is necessary for placode formation and, consequently, dermal organization. The first permissive dermal signaling is a combination of factors: WNT, for β-catenin stabilization; and others that initiate *FGF2* and *BMP7* expression in the epidermis (Harris et al., 2004). The loss of either *FGF2*, in the *Scaleless* mutant, or *BMP7* function in the epidermis leads to feather defects (Song et al., 1996; Song et al., 2004; Viallet et al., 1998; Harris et al., 2004). Diffusible epidermal chemoattractant factors, such as BMP7 and FGF2 (Song et al., 2004), trigger the migration of dermal cells to the placodal area. Then, the dermal expression of *BMP7*, which is regulated by a placodal WNT signal (Harris et al., 2004), enhances this process. *BMP2* expression, in the placode and then in the dermal condensation (Noramly and Morgan, 1998), could modify dermal integrin expression and regulate the splicing of fibronectin EIIIA; both of these events lead to a decrease of dermal cell migration capabilities, signifying the second phase of follicular domain delimitation. Two other facts contribute to the limitation of the feather primordium diameter. The induction by BMP7 of follistatin expression (Patel et al., 1999) leads to a lateral inhibition of BMP signaling, which is reinforced by the expression of *DRM*/gremlin (Bardot et al., 2004). Finally, the induction of the Notch system, after *BMP2* expression (F.M., unpublished), stabilizes (Chen et al., 1997) the follicular domain identity by strengthening its boundaries.

Our main conclusion is that different members of the BMP family play at least two important roles in chick dermal condensation formation. First, epidermal, and then dermal, BMP7 activates the migration of dermal fibroblasts to the appendage domain via chemotaxis. Second, epidermal, and then dermal, BMP2 stops the migration, probably by regulating the expression of integrin and fibronectin EIIIA. This effect, later reinforced by the expression of *BMP4* in the dermis, may lead to the limitation of dermal condensation size. Moreover, the activation of target genes, such as members of the ID and MSX families, suggests a subtle cell transcriptome regulation in the primordium, caused by the transcriptional inhibitor role of the ID factors (Kreider et al., 1992; Miyazono and Miyazawa, 2002) and the transcriptional activator role of the MSX factors (Lallemand et al., 2005; Ramos and Robert, 2005) during the continuation of feather morphogenesis.

We are grateful to Dr M. O'Guin, Dr I. Olivera-Martinez, Dr D. J. Pearton, Dr T. T. Sun and Dr M. Tummers for critical reading of the manuscript. We thank Dr N. T. Chartier for the FACS experiments and Mrs B. Peyrusse for the iconography. F.M. was the recipient of a doctoral fellowship from the French Ministère de la Recherche. This work was supported by the CNRS and by INSERM. This article is dedicated to the memory of Loïc Forest.

Supplementary material

Supplementary material for this article is available at
http://dev.biologists.org/cgi/content/full/135/16/2797/DC1

References

Bardot, B., Lecoin, L., Fliniaux, I., Huillard, E., Marx, M. and Viallet, J. P. (2004). Drm/Gremlin, a BMP antagonist, defines the interbud region during feather development. *Int. J. Dev. Biol.* **48**, 149-156.

Botchkarev, V. A. (2003). Bone morphogenetic proteins and their antagonists in skin and hair follicle biology. *J. Invest. Dermatol.* **120**, 36-47.

Chen, C. W., Jung, H. S., Jiang, T. X. and Chuong, C. M. (1997). Asymmetric expression of Notch/Delta/Serrate is associated with the anterior-posterior axis of feather buds. *Dev. Biol.* **188**, 181-187.

Chuong, C. M. (1993). The making of a feather: homeoproteins, retinoids and adhesion molecules. *BioEssays* **15**, 513-521.

Chuong, C. M. (1998). Molecular Basis of Epithelial Appendage Morphogenesis. Austin, TX: Landes Bioscience.

Chuong, C. M., Widelitz, R. B., Ting-Berreth, S. and Jiang, T. X. (1996). Early events during avian skin appendage regeneration: dependence on epithelial-mesenchymal interaction and order of molecular reappearance. *J. Invest. Dermatol.* **107**, 639-646.

Cruywagen, G. C., Maini, P. K. and Murray, J. D. (1992). Sequential pattern formation in a model for skin morphogenesis. *IMA J. Math. Appl. Med. Biol.* **9**, 227-248.

Desbiens, X., Queva, C., Jaffredo, T., Stehelin, D. and Vandenbunder, B. (1991). The relationship between cell proliferation and the transcription of the nuclear oncogenes c-myc, c-myb and c-ets-1 during feather morphogenesis in the chick embryo. *Development* **111**, 699-713.

Dhouailly, D. (1977). Dermo-epidermal interactions during morphogenesis of cutaneous appendages in amniotes. In *Frontier Matrix Biology*, vol. 4 (ed. L. Robert), pp. 85-91. Paris: Creteil.
Dhouailly, D. (1984). Specification of feather and scale patterns. In *Pattern formation* (ed. G. Malacinski and S. Bryant), pp. 581-601. London: Macmillan.
Fliniaux, I., Viallet, J. P. and Dhouailly, D. (2004). Signaling dynamics of feather tract formation from the chick somatopleure. *Development* **131**, 3955-3966.
Gierer, A. and Meinhardt, H. (1972). A theory of biological pattern formation. *Kybernetik* **12**, 30-39.
Hamburger, V. and Hamilton, H. L. (1951). A series of normal stages in the development of the chick embryo. *J. Morphol.* **88**, 49-92.
Harris, M. P., Linkhart, B. L. and Fallon, J. F. (2004). Bmp7 mediates early signaling events during induction of chick epidermal organs. *Dev. Dyn.* **231**, 22-32.
Hazama, M., Aono, A., Ueno, N. and Fujisawa, Y. (1995). Efficient expression of a heterodimer of bone morphogenetic protein subunits using a baculovirus expression system. *Biochem. Biophys. Res. Commun.* **209**, 859-866.
Hollnagel, A., Oehlmann, V., Heymer, J., Ruther, U. and Nordheim, A. (1999). Id genes are direct targets of bone morphogenetic protein induction in embryonic stem cells. *J. Biol. Chem.* **274**, 19838-19845.
Houghton, L., Lindon, C. and Morgan, B. A. (2005). The ectodysplasin pathway in feather tract development. *Development* **132**, 863-872.
Jaspers, M., Wu, R. R., Van der Schueren, B. and Cassiman, J. J. (1995). Localization of alpha 4m integrin at sites of mesenchyme condensation during embryonic mouse development. *Differentiation* **59**, 79-86.
Jiang, T. X. and Chuong, C. M. (1992). Mechanism of skin morphogenesis. I. Analyses with antibodies to adhesion molecules tenascin, N-CAM, and integrin. *Dev. Biol.* **150**, 82-98.
Jiang, T. X., Jung, H. S., Widelitz, R. B. and Chuong, C. M. (1999). Self-organization of periodic patterns by dissociated feather mesenchymal cells and the regulation of size, number and spacing of primordia. *Development* **126**, 4997-5009.
Jiang, T. X., Widelitz, R. B., Shen, W. M., Will, P., Wu, D. Y., Lin, C. M., Jung, H. S. and Chuong, C. M. (2004). Integument pattern formation involves genetic and epigenetic controls: feather arrays simulated by digital hormone models. *Int. J. Dev. Biol.* **48**, 117-135.
Jung, H. S., Francis-West, P. H., Widelitz, R. B., Jiang, T. X., Ting-Berreth, S., Tickle, C., Wolpert, L. and Chuong, C. M. (1998). Local inhibitory action of BMPs and their relationships with activators in feather formation: implications for periodic patterning. *Dev. Biol.* **196**, 11-23.
Kee, Y. and Bronner-Fraser, M. (2001). Id4 expression and its relationship to other Id genes during avian embryonic development. *Mech. Dev.* **109**, 341-345.
Kreider, B. L., Benezra, R., Rovera, G. and Kadesch, T. (1992). Inhibition of myeloid differentiation by the helix-loop-helix protein Id. *Science* **255**, 1700-1702.
Lallemand, Y., Nicola, M. A., Ramos, C., Bach, A., Cloment, C. S. and Robert, B. (2005). Analysis of Msx1; Msx2 double mutants reveals multiple roles for Msx genes in limb development. *Development* **132**, 3003-3014.
Lauffenburger, D. A. (1996). Cell motility. Making connections count. *Nature* **383**, 390-391.
Lee, D. H., Park, B. J., Lee, M. S., Lee, J. W., Kim, J. K., Yang, H. C. and Park, J. C. (2006). Chemotactic migration of human mesenchymal stem cells and MC3T3-E1 osteoblast-like cells induced by COS-7 cell line expressing rhBMP-7. *Tissue Eng.* **12**, 1577-1586.
Manabe, R., Ohe, N., Maeda, T., Fukuda, T. and Sekiguchi, K. (1997). Modulation of cell-adhesive activity of fibronectin by the alternatively spliced EDA segment. *J. Cell Biol.* **139**, 295-307.
Manabe, R., Oh-e, N. and Sekiguchi, K. (1999). Alternatively spliced EDA segment regulates fibronectin-dependent cell cycle progression and mitogenic signal transduction. *J. Biol. Chem.* **274**, 5919-5924.
Mauger, A., Demarchez, M., Herbage, D., Grimaud, J. A., Druguet, M., Hartmann, D. and Sengel, P. (1982). Immunofluorescent localization of collagen types I and III, and of fibronectin during feather morphogenesis in the chick embryo. *Dev. Biol.* **94**, 93-105.
Mayerson, P. L. and Fallon, J. F. (1985). The spatial pattern and temporal sequence in which feather germs arise in the white Leghorn chick embryo. *Dev. Biol.* **109**, 259-267.
Michon, F., Charveron, M. and Dhouailly, D. (2007). Dermal condensation formation in the chick embryo: requirement for integrin engagement and subsequent stabilization by a possible notch/integrin interaction. *Dev. Dyn.* **236**, 755-768.
Miyazono, K. (1999). Signal transduction by bone morphogenetic protein receptors: functional roles of Smad proteins. *Bone* **25**, 91-93.
Miyazono, K. and Miyazawa, K. (2002). Id: a target of BMP signaling. *Sci. STKE* **2002**, PE40.
Miyazono, K., Maeda, S. and Imamura, T. (2005). BMP receptor signaling: transcriptional targets, regulation of signals, and signaling cross-talk. *Cytokine Growth Factor Rev.* **16**, 251-263.
Noramly, S. and Morgan, B. A. (1998). BMPs mediate lateral inhibition at successive stages in feather tract development. *Development* **125**, 3775-3787.
Noramly, S., Freeman, A. and Morgan, B. A. (1999). beta-catenin signaling can initiate feather bud development. *Development* **126**, 3509-3521.
Norton, P. A. and Hynes, R. O. (1987). Alternative splicing of chicken fibronectin in embryos and in normal and transformed cells. *Mol. Cell. Biol.* **7**, 4297-4307.
Noveen, A., Jiang, T. X., Ting-Berreth, S. A. and Chuong, C. M. (1995). Homeobox genes Msx-1 and Msx-2 are associated with induction and growth of skin appendages. *J. Invest. Dermatol.* **104**, 711-719.
Ogata, T., Wozney, J. M., Benezra, R. and Noda, M. (1993). Bone morphogenetic protein 2 transiently enhances expression of a gene, Id (inhibitor of differentiation), encoding a helix-loop-helix molecule in osteoblast-like cells. *Proc. Natl. Acad. Sci. USA* **90**, 9219-9222.
Olivera-Martinez, I., Thelu, J., Teillet, M. A. and Dhouailly, D. (2001). Dorsal dermis development depends on a signal from the dorsal neural tube, which can be substituted by Wnt-1. *Mech. Dev.* **100**, 233-244.
Olivera-Martinez, I., Missier, S., Fraboulet, S., Thelu, J. and Dhouailly, D. (2002). Differential regulation of the chick dorsal thoracic dermal progenitors from the medial dermomyotome. *Development* **129**, 4763-4772.
Ozeki, N., Jethanandani, P., Nakamura, H., Ziober, B. L. and Kramer, R. H. (2007). Modulation of satellite cell adhesion and motility following BMP2-induced differentiation to osteoblast lineage. *Biochem. Biophys. Res. Commun.* **353**, 54-59.
Painter, K. J., Maini, P. K. and Othmer, H. G. (1999). Stripe formation in juvenile Pomacanthus explained by a generalized Turing mechanism with chemotaxis. *Proc. Natl. Acad. Sci. USA* **96**, 5549-5554.
Patel, K., Makarenkova, H. and Jung, H. S. (1999). The role of long range, local and direct signalling molecules during chick feather bud development involving the BMPs, follistatin and the Eph receptor tyrosine kinase Eph-A4. *Mech. Dev.* **86**, 51-62.
Pummila, M., Fliniaux, I., Jaatinen, R., James, M. J., Laurikkala, J., Schneider, P., Thesleff, I. and Mikkola, M. L. (2007). Ectodysplasin has a dual role in ectodermal organogenesis: inhibition of Bmp activity and induction of Shh expression. *Development* **134**, 117-125.
Ramos, C. and Robert, B. (2005). msh/Msx gene family in neural development. *Trends Genet.* **21**, 624-632.
Rouzankina, I., Abate-Shen, C. and Niswander, L. (2004). Dlx genes integrate positive and negative signals during feather bud development. *Dev. Biol.* **265**, 219-233.
Scaal, M., Prols, F., Fuchtbauer, E. M., Patel, K., Hornik, C., Kohler, T., Christ, B. and Brand-Saberi, B. (2002). BMPs induce dermal markers and ectopic feather tracts. *Mech. Dev.* **110**, 51-60.
Sebald, W. and Mueller, T. D. (2003). The interaction of BMP-7 and ActRII implicates a new mode of receptor assembly. *Trends Biochem. Sci.* **28**, 518-521.
Sengel, P. (1976). *Morphogenesis of Skin*. Cambridge: Cambridge University Press.
Song, H., Wang, Y. and Goetinck, P. F. (1996). Fibroblast growth factor 2 can replace ectodermal signaling for feather development. *Proc. Natl. Acad. Sci. USA* **93**, 10246-10249.
Song, H. K., Lee, S. H. and Goetinck, P. F. (2004). FGF-2 signaling is sufficient to induce dermal condensations during feather development. *Dev. Dyn.* **231**, 741-749.
Sotobori, T., Ueda, T., Myoui, A., Yoshioka, K., Nakasaki, M., Yoshikawa, H. and Itoh, K. (2006). Bone morphogenetic protein-2 promotes the haptotactic migration of murine osteoblastic and osteosarcoma cells by enhancing incorporation of integrin beta1 into lipid rafts. *Exp. Cell Res.* **312**, 3927-3938.
Tao, H., Yoshimoto, Y., Yoshioka, H., Nohno, T., Noji, S. and Ohuchi, H. (2002). FGF10 is a mesenchymally derived stimulator for epidermal development in the chick embryonic skin. *Mech. Dev.* **116**, 39-49.
Turing, A. M. (1952). The chemical basis of morphogenesis. *Phil. Trans. R. Soc. Lond. B Biol. Sci.* **237**, 37-72.
Viallet, J. P., Prin, F., Olivera-Martinez, I., Hirsinger, E., Pourquié, O. and Dhouailly, D. (1998). Chick Delta-1 gene expression and the formation of the feather primordia. *Mech. Dev.* **72**, 159-168.
Wessells, N. K. (1965). Morphology and proliferation during early feather development. *Dev. Biol.* **12**, 131-153.
Widelitz, R. B., Jiang, T. X., Noveen, A., Chen, C. W. and Chuong, C. M. (1996). FGF induces new feather buds from developing avian skin. *J. Invest. Dermatol.* **107**, 797-803.
Wilkinson, D. G. and Nieto, M. A. (1993). Detection of messenger RNA by in situ hybridization to tissue sections and whole mounts. *Meth. Enzymol.* **225**, 361-373.
Zhang, L., Deng, M., Parthasarathy, R., Wang, L., Mongan, M., Molkentin, J. D., Zheng, Y. and Xia, Y. (2005). MEKK1 transduces activin signals in keratinocytes to induce actin stress fiber formation and migration. *Mol. Cell. Biol.* **25**, 60-65.
Zou, H. and Niswander, L. (1996). Requirement for BMP signaling in interdigital apoptosis and scale formation. *Science* **272**, 738-741.

Table S1. Parameters for the mathematical model

Parameters	Values
N	2.6
Q	0.95
D_u	0.00625
D_v	0.13333
D_n	0.00007
X	0.00008
k_u	15
k_v	35
k_p	0.006
k_d	0.005
$c1$	100
$c2$	40
$c3$	6
$c4$	4500

Functions	Expression	
$n_{1,0}(x)$	$0.25+1.7*\exp(-(x)^2*5)+0.2*\exp(-(x)^2*200)$	Sequential formation
$n_{2,0}(x)$	$0.05+2*\exp(-(x)^2*200)$	Sequential formation
$n_{1,0}(x)$	0	Impact of cell initial density
$n_{2,0}(x,y)$	q+fluctuations	Impact of cell initial density

Presented are the various constants and parameters used in the numerical resolution of the mathematical model.